Hydrodynamic spin states

Anand U. Oza, Rodolfo R. Rosales, and John W. M. Bush

Articles you may be interested in

The interaction of a walking droplet and a submerged pillar: From scattering to the logarithmic spiral
Chaos: An Interdisciplinary Journal of Nonlinear Science **28**, 096105 (2018); 10.1063/1.5031022

Bouncing droplet dynamics above the Faraday threshold
Chaos: An Interdisciplinary Journal of Nonlinear Science **28**, 096107 (2018); 10.1063/1.5031426

Hong–Ou–Mandel-like two-droplet correlations
Chaos: An Interdisciplinary Journal of Nonlinear Science **28**, 096104 (2018); 10.1063/1.5032114

Faraday-Talbot effect: Alternating phase and circular arrays
Chaos: An Interdisciplinary Journal of Nonlinear Science **28**, 096101 (2018); 10.1063/1.5031442

Standard map-like models for single and multiple walkers in an annular cavity
Chaos: An Interdisciplinary Journal of Nonlinear Science **28**, 096102 (2018); 10.1063/1.5033949

Bouncing ball on a vibrating periodic surface
Chaos: An Interdisciplinary Journal of Nonlinear Science **28**, 096103 (2018); 10.1063/1.5023397

Hydrodynamic spin states

Anand U. Oza,[1,a)] Rodolfo R. Rosales,[2] and John W. M. Bush[2]

[1]*Department of Mathematical Sciences, New Jersey Institute of Technology, Newark, New Jersey 07102, USA*
[2]*Department of Mathematics, Massachusetts Institute of Technology, Cambridge, Massachusetts 02139, USA*

We present the results of a theoretical investigation of hydrodynamic spin states, wherein a droplet walking on a vertically vibrating fluid bath executes orbital motion despite the absence of an applied external field. In this regime, the walker's self-generated wave force is sufficiently strong to confine the walker to a circular orbit. We use an integro-differential trajectory equation for the droplet's horizontal motion to specify the parameter regimes for which the innermost spin state can be stabilized. Stable spin states are shown to exhibit an analog of the Zeeman effect from quantum mechanics when they are placed in a rotating frame. *Published by AIP Publishing.* https://doi.org/10.1063/1.5034134

An oil droplet may walk on the surface of a vertically vibrated fluid bath, propelled by its self-generated wave-field. The resulting hydrodynamic pilot-wave system has received considerable attention from the scientific community, as it exhibits features that were once thought to be peculiar to the microscopic quantum realm. We here present the results of a theoretical investigation of hydrodynamic spin states, in which the walker executes circular orbits in the absence of an external field. While spin states have not yet been observed in the laboratory, we specify the parameter regimes in which they could be stabilized in a generalized pilot-wave framework.

I. INTRODUCTION

Millimetric oil droplets bouncing on a vibrating fluid bath exhibit behavior reminiscent of quantum phenomena, such as tunneling,[1] orbital quantization[2] and level-splitting,[3] double quantization in a harmonic potential,[4] and quantum corrals.[5] These "walkers" have recently attracted considerable interest from the scientific community, as they offer an intriguing visualization of wave-particle coupling on a macroscopic scale, and represent the first realization of the pilot-wave dynamics envisioned by Louis de Broglie. The interested reader is referred to comprehensive review articles concerning this hydrodynamic pilot-wave system.[6,7]

The experiments of Fort *et al.*[2] and then Harris and Bush[8] showed that droplets walking on a rotating bath execute circular orbits in the rotating frame of reference. Provided the vibrational forcing of the bath is sufficiently large, the orbital radii are quantized on the half-Faraday wavelength $\lambda_F/2$, with λ_F being the wavelength of the surface waves generated by the walker. Since the Coriolis force $-2m\mathbf{\Omega} \times \dot{\mathbf{x}}$ acting on a particle of mass m in a frame rotating with angular frequency $\mathbf{\Omega}$ is analogous in form to the Lorentz force $-q\mathbf{B} \times \dot{\mathbf{x}}$ acting on a particle of charge q in a uniform magnetic field $\mathbf{B}$, Fort *et al.*[2] proposed an analogy between the walker's quantized orbits and quantum mechanical Landau levels.[9] Eddi *et al.*[3] extended the analogy using pairs of walkers orbiting

each other in a rotating frame. Specifically, they found that orbits rotating in the same sense as the bath had slightly larger radii than counterrotating ones, the discrepancy increasing roughly linearly as the bath rotation rate was increased. This phenomenon is analogous to the Zeeman effect[9] in quantum mechanics, wherein an electron's degenerate energy level splits in the presence of a uniform magnetic field. Circular orbits were also found to be quantized when the walker is subjected to a harmonic potential.[4]

Building on the theoretical developments of Moláček and Bush,[10,11] Oza *et al.*[12] developed an integro-differential trajectory equation for a walker's horizontal motion, which exhibited good agreement[13] with experimental data on orbital trajectories in a rotating frame[8] and harmonic potential.[14] Multiple stable orbital solutions were found to coexist for identical values of the applied external field and were separated by unstable solutions, which provides rationale for the observed quantization of orbits. Moreover, Oza *et al.*[13] demonstrated the possibility of *hydrodynamic spin states*, wherein a walker executes uniform circular motion in its self-induced wavefield despite the absence of an external force. Solutions corresponding to such states were found to arise at relatively large values of the bath's forcing acceleration, when the wave force is sufficiently strong to confine the walker. However, these spin states were found to be unstable in the parameter regime explored experimentally by Fort *et al.*[2] and Harris and Bush.[8]

Labousse *et al.*[15] studied the stability of spin states both experimentally and numerically. In their experiments, the authors placed a walker in a harmonic potential, causing the walker to execute a circular orbit with radius $r_0/\lambda_F \approx 0.37$. They slowly turned off the harmonic potential and found that the circular orbit could persist for up to six orbital periods in the absence of an external force before destabilizing into a rectilinear walking state. The authors then conducted numerical simulations of the walker's dynamics using a discrete-time iterated map. They chose their simulation parameters to roughly match those corresponding to their experiments and found that spin states were stable above a critical value of the bath forcing acceleration. These states persisted even in the presence of a small amount of controlled noise,

a)oza@njit.edu

suggesting that the instability of spin states in their experiments can be attributed to relatively large experimental noise. The simulations also revealed the possibility of wobbling spin states, wherein the orbital radius of curvature exhibits a temporal oscillation incommensurate with the orbital frequency.

The work of Labousse *et al.*[15] does not address the stability of spin states analytically. Moreover, they do not examine the dependence of the spin states' stability properties on the orbital radius nor the experimental parameters. We here use the integro-differential trajectory equation derived by Oza *et al.*[12,13] to assess the stability of spin states analytically and thus determine the parameter regimes in which they are stable and unstable.

The paper is organized as follows. In Sec. II, we review the integro-differential trajectory equation and recast it in a new dimensionless form. The existence and stability of spin states is treated in Sec. III. A discussion of our results and future directions is given in Sec. IV.

II. GENERALIZED PILOT-WAVE MODEL

Consider a droplet of mass m and radius R, in the presence of a gravitational acceleration g, bouncing on the surface of a vertically vibrating bath of the same fluid. The fluid bath has surface tension σ, density ρ, kinematic viscosity ν, and depth H. It is subject to a vertical acceleration $\gamma \cos(2\pi ft)$ and a uniform rotation of angular frequency $\mathbf{\Omega} = \Omega\hat{z}$. Provided $\gamma < \gamma_F$, with γ_F being the Faraday instability threshold,[16] the surface of the bath remains flat. Following Moláček and Bush,[11] we assume that the drop is propelled by a wave force proportional to the local slope of the wave field and resisted by the drag induced during impact and flight. We also assume the droplet to be a "resonant walker," in that its bouncing period $T_F = 2/f$ is equal to that of the least stable Faraday mode of the fluid bath. Averaging the horizontal forces over the bouncing period yields an integro-differential trajectory equation[12,13] for the walker's horizontal position $\mathbf{x}_p(t)$:

$$m\ddot{\mathbf{x}}_p + D\dot{\mathbf{x}}_p = -mg\nabla h[\mathbf{x}_p(t), t] - 2m\mathbf{\Omega} \times \dot{\mathbf{x}}_p,$$
$$h(\mathbf{x}, t) = \frac{A}{T_F}\int_{-\infty}^{t} J_0\left[k_F\left|\mathbf{x} - \mathbf{x}_p(s)\right|\right] e^{-(t-s)/T_M}\, ds, \quad (1)$$

where J_0 is a Bessel function of the first kind. The drag coefficient D, memory time T_M,[17] and wave amplitude A are given by the formulas[11]

$$D = Cmg\sqrt{\frac{\rho R}{\sigma}} + 6\pi\mu_a R\left(1 + \frac{\rho_a g R}{12\mu_a f}\right),$$
$$T_M = \frac{T_d}{1 - \gamma/\gamma_F}$$
$$\text{and}\quad A = \frac{\sqrt{8\pi\nu_e T_F}}{3}\frac{(k_F R)^3}{3k_F^2\sigma/(\rho g) + 1}\sin\Phi. \quad (2)$$

Here, T_d is the viscous decay time of the surface waves in the absence of forcing, C is a dimensionless drag constant, ρ_a and μ_a are the density and dynamic viscosity of air, respectively, ν_e is the bath's effective kinematic viscosity,[11] and $\sin\Phi$ is the sine of the droplet's impact phase. The Faraday wavenumber $k_F = 2\pi/\lambda_F$ may be approximated by the water-wave dispersion relation $(\pi f)^2 = (gk_F + \sigma k_F^3/\rho)\tanh(k_F H)$

for this system[11] and may generally be calculated using the method presented by Kumar.[18] Note that, as $\gamma \to \gamma_F$ from below, the waves become progressively more persistent, so the walker's trajectory is influenced more strongly by its distant past. For the sake of simplicity, we neglect the effect of spatial damping,[19,20] which is the experimentally observed exponential decay of the surface waves in the far field. We also neglect the dependence of the impact phase $\sin\Phi$ on both the forcing acceleration γ and the instantaneous wave height $h[\mathbf{x}_p(t), t]$, an effect that has been shown to stabilize both the orbital[21] and promenade[22] modes executed by pairs of walkers in the absence of an external force.

We first nondimensionalize the trajectory equation using the Faraday wavelength and memory time, and so let $\mathbf{x} \to k_F\mathbf{x}$, $t \to t/T_M$, and $\mathbf{\Omega} \to 2m\mathbf{\Omega}/D$ in Eq. (1). We thus obtain the dimensionless trajectory equation

$$\kappa\ddot{\mathbf{x}}_p + \dot{\mathbf{x}}_p = -\beta\nabla h[\mathbf{x}_p(t), t] - \mathbf{\Omega} \times \dot{\mathbf{x}}_p,$$
$$h(\mathbf{x}, t) = \int_{-\infty}^{t} J_0\left[\left|\mathbf{x} - \mathbf{x}_p(s)\right|\right] e^{-(t-s)}\, ds, \quad (3)$$

where $\kappa = m/DT_M$ and $\beta = mgAk_F^2 T_M^2/DT_F$.

A more convenient dimensionless form may be obtained by noting that, in the absence of rotation ($\Omega = 0$), the walking threshold occurs at $\beta = 2$. That is, the critical forcing acceleration $\gamma = \gamma_W$ above which the bouncing state $\mathbf{x}_p(t) = 0$ destabilizes into a steady walking state is[12]

$$\frac{\gamma_W}{\gamma_F} = 1 - \sqrt{\frac{mgAk_F^2 T_d^2}{2DT_F}}. \quad (4)$$

Defining the dimensionless parameters

$$\Gamma = \frac{\gamma - \gamma_W}{\gamma_F - \gamma_W}, \quad \kappa_0 = k_F\left(\frac{m}{D}\right)^{3/2}\sqrt{\frac{gA}{2T_F}}, \quad (5)$$

we find that $\beta = 2/(1-\Gamma)^2$ and $\kappa = \kappa_0(1-\Gamma)$. We thus obtain the dimensionless trajectory equation[6]

$$\kappa_0(1-\Gamma)\ddot{\mathbf{x}}_p + \dot{\mathbf{x}}_p = -\frac{2}{(1-\Gamma)^2}\nabla h[\mathbf{x}_p(t), t] - \mathbf{\Omega} \times \dot{\mathbf{x}}_p, \quad (6)$$

where the equation for h is identical to that in Eq. (3). The parameter Γ is a dimensionless forcing acceleration in the interval $0 \leq \Gamma < 1$, with $\Gamma = 0$ being the walking threshold and $\Gamma = 1$ the Faraday threshold. The parameter κ_0 plays the role of a dimensionless mass. We find that $\kappa_0 = O(1)$ for the parameter values typically used in prior experiments.[11,23] Specifically, for a walker of radius $R \approx 0.4$ mm with impact phase $\sin\Phi \approx 0.2$ and drag factor $C = 0.17$, we find that $0.9 \lesssim \kappa_0 \lesssim 2.2$ for the parameter ranges $20\,\text{Hz} \leq f \leq 80\,\text{Hz}$ and $20\,\text{cSt} \leq \nu \leq 50\,\text{cSt}$.

The advantage of Eq. (6) over Eq. (3) is that the fluid parameters are all contained within the single parameter κ_0. The full range of Γ may be accessed simply by tuning the dimensional forcing acceleration γ. This makes Eq. (6) ideal for conducting parametric studies beyond the regimes encompassed by prior experiments or accessible in the laboratory.

III. EXISTENCE AND STABILITY OF SPIN STATES

Equation (6) admits orbital solutions $x_p(t) = r_0(\cos \omega t, \sin \omega t)$, wherein a walker executes uniform circular motion in the rotating frame of reference. The orbital radius r_0 and frequency ω are solutions of the pair of algebraic equations[13]

$$-\kappa_0(1-\Gamma)r_0\omega^2 - \Omega r_0\omega$$
$$= \frac{2}{(1-\Gamma)^2} \int_0^\infty J_1\left(2r_0 \sin \frac{\omega z}{2}\right) \sin \frac{\omega z}{2} e^{-z} \, dz, \quad (7a)$$

$$r_0\omega = \frac{2}{(1-\Gamma)^2} \int_0^\infty J_1\left(2r_0 \sin \frac{\omega z}{2}\right) \cos \frac{\omega z}{2} e^{-z} \, dz. \quad (7b)$$

The first equation (7a) expresses the force balance in the radial direction, which reflects a competition between the walker's inertia, the Coriolis force, and the radial component of the wave force. The second equation (7b) expresses the force balance in the azimuthal direction of motion, in which the walker's drag balances the propulsive wave force. The solutions of Eq. (7) exhibit good agreement[13] with experimental data[8] of orbital trajectories in a rotating frame. In particular, the orbital radii r_0 are quantized provided the forcing acceleration Γ is sufficiently large, an effect first observed experimentally by Fort et al.[2]

Oza et al.[13] observed that the solutions to Eq. (7) occur in pairs (Ω, r_0, ω) and $(-\Omega, r_0, -\omega)$, where ω and Ω have opposite signs for moderate values of the forcing acceleration Γ. They showed that, as Γ is increased progressively, these two branches of solutions intersect at points for which $\Omega = 0$, which correspond to hydrodynamic spin states. We seek spin state solutions by setting $\Omega = 0$ in Eq. (7a). These solutions may be classified by their behavior as $\Gamma \to 1$ from below. In this limit, it can be shown[13,15] that there is a spin state solution with orbital radius $r_0 = \rho_n$ for each zero $\rho_n > 0$ of J_0. We neglect the spin state solutions corresponding to the zeros of J_1, as such states were previously shown to be unstable to a non-oscillatory instability.[13] The zeros of J_0 are ordered as $0 < \rho_0 < \rho_1 < \cdots$, so $n = 0$ denotes the innermost spin state. Each of these solutions persists for $\Gamma_n(\kappa_0) \leq \Gamma \leq 1$, where the critical curves $\Gamma = \Gamma_n(\kappa_0)$ are indicated by the solid lines in Fig. 1. In order to find the spin states, we solve the equations using an iterative root-finding program in Matlab with $r_0 = \rho_n$ and $\omega = u_0/r_0$ as the initial guess, where u_0 is the free walking speed of a walker.[12] As shown in Fig. 1, Γ_n increases with both orbit order n and dimensionless mass κ_0, since a larger wave force is required to sustain both larger orbits and orbiting walkers with more inertia.

We now assess the stability of the spin state solutions using the procedure described by Oza et al.,[13] which we summarize briefly. Equation (6) is linearized around the orbital solution, and the linear equations are solved using Laplace transforms. It was shown that the eigenvalues of the linear stability problem are given by the roots of the function $F(s)$, whose functional form is given in the Appendix. As described in the Appendix, we implement a numerical method based on the argument principle from complex analysis to find the roots of $F(s)$ in the complex plane. The orbital solution is stable if all of the roots satisfy $\mathrm{Re}(s) < 0$ and is unstable otherwise.
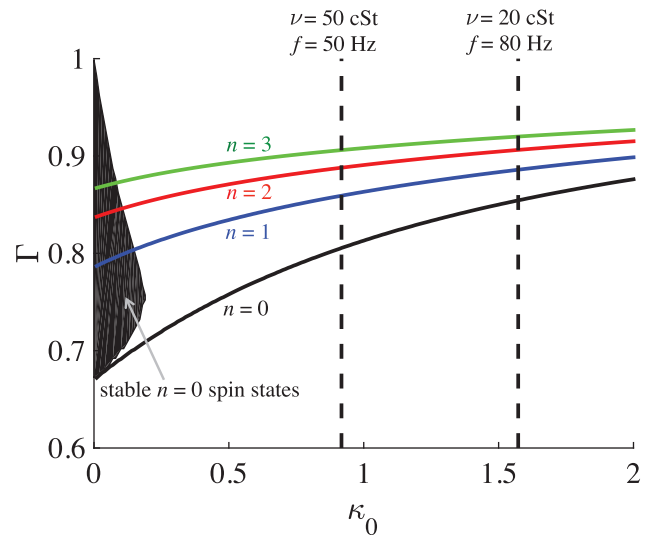

FIG. 1. Existence and stability of spin states within the generalized pilot-wave framework. The solid lines indicate the values of $\Gamma = \Gamma_n(\kappa_0)$ above which spin states exist, the colors denoting different orbit orders n. The solid black region indicates the region of parameter space in which $n = 0$ spin states are stable. The dashed vertical black lines indicate the values of κ_0 corresponding to walkers of radius $R = 0.4$ mm, impact phase $\sin \Phi = 0.2$, and drag factor $C = 0.17$, for two different values of kinematic viscosity ν and forcing frequency f. These parameters correspond to those typically used in experiments.[11,23]

Our stability analysis shows that there is a region in the (κ_0, Γ) plane for which $n = 0$ spin states are stable, indicated by the black region in Fig. 1. As one crosses the stability boundary into the unstable region, the spin states destabilize via an oscillatory instability, as a complex-conjugate pair of roots of $F(s)$ crosses the imaginary axis. Our model (6) predicts that spin states for $n \geq 1$ are unstable for all values of κ_0 and Γ. The stability of the $n = 0$ spin states was confirmed by numerically solving the trajectory equation (6), and the circular orbits were observed to persist over a simulation time exceeding 300 orbital periods. The numerical method, which is described in detail elsewhere,[24] uses an Adams-Bashforth fourth-order time-stepping scheme combined with Simpson's rule for the integration. The initial conditions for the walker x_p and the wave field h correspond to those defined by the orbital solution in Eq. (7).

For the values of (κ_0, Γ) corresponding to stable $n = 0$ spin states, we also observe an analog Zeeman effect, as shown in Fig. 2. Specifically, with (κ_0, Γ) fixed, we find the solutions to Eq. (7) as functions of Ω. Since multiple orbital solutions may exist for a single value of Ω, we sweep the orbital radius r_0 and find the corresponding values of the orbital frequency ω and bath rotation rate Ω that satisfy Eq. (7). The two branches in Fig. 2(a) are accessed by changing the sign of the initial guess for ω, with $\omega > 0$ corresponding to the left branch and $\omega < 0$ to the right. The solutions are color-coded according to their stability properties, as is determined by the root s^* of $F(s)$ with the largest real part. Blue denotes stable orbits, for which $\mathrm{Re}(s^*) < 0$. Red denotes unstable orbits that undergo a non-oscillatory instability [$\mathrm{Re}(s^*) > 0$, $\mathrm{Im}(s^*) = 0$], and green denotes orbits that undergo an oscillatory instability [$\mathrm{Re}(s^*) > 0$, $\mathrm{Im}(s^*) \neq 0$].
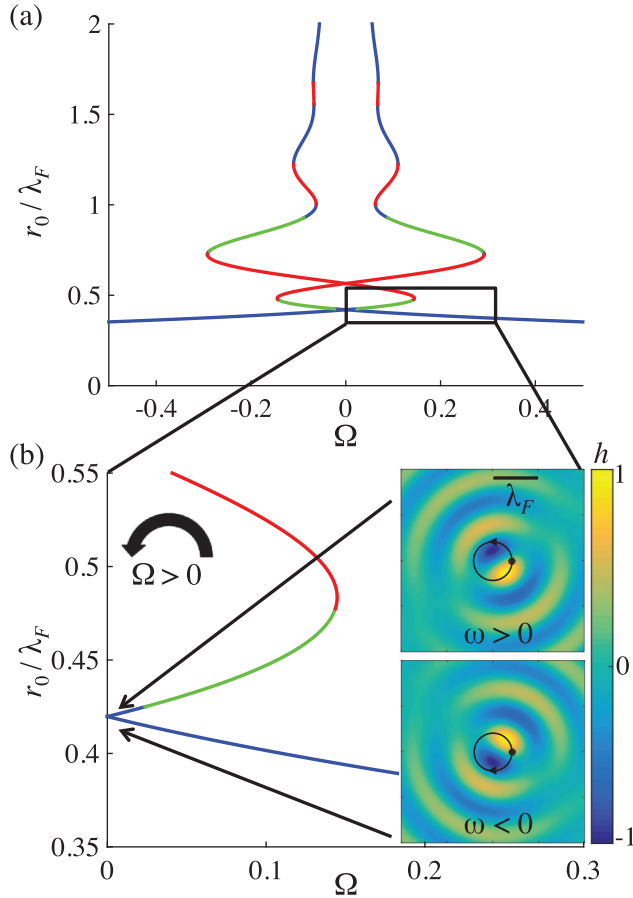
FIG. 2. Analog of Zeeman splitting observed in a generalized pilot-wave theory with $\kappa_0 = 0.1$ and $\Gamma = 0.75$. The two spin states at $\Omega = 0$, with orbital frequencies $\omega > 0$ and $\omega < 0$, split into solutions of different radii r_0 as the dimensionless bath rotation rate Ω is increased from zero. The insets show the wave fields $h(\boldsymbol{x})$ (arbitrary units) corresponding to orbits for $\Omega = 0.02$, as given by Eq. (3), plotted in a reference frame rotating with the walker (black dot). The orbital solutions are color-coded according to their stability, determined by the root s^* of $F(s)$ with the largest real part. Blue denotes stable orbits, for which $\mathrm{Re}(s^*) < 0$. Red denotes unstable orbits that undergo a nonoscillatory instability [$\mathrm{Re}(s^*) > 0$, $\mathrm{Im}(s^*) = 0$], and green denotes orbits that undergo an oscillatory instability [$\mathrm{Re}(s^*) > 0$, $\mathrm{Im}(s^*) \neq 0$].

The two $n = 0$ spin state solutions for $\Omega = 0$ have the same radius r_0 and orbital frequencies of opposite signs, $\omega = \pm\omega_0$. As shown in Fig. 2(b), the co-rotating solution $\omega > 0$ increases in radius as Ω is progressively increased from zero, whereas the counter-rotating solution $\omega < 0$ decreases in radius, both solutions remaining stable for a range of Ω values. While this analog Zeeman effect was hypothesized by Oza et al.,[13] the corresponding orbital solutions were shown to be unstable. Indeed, the value of $\kappa_0 \approx 2$ used in that work was too large to support spin states, as it was based on the experimental parameters reported by Harris and Bush.[8] We note that this splitting is similar in form to that reported by Eddi et al.[3] for orbiting pairs of walkers in a rotating frame.

Might it be possible to observe stable $n = 0$ spin states in the laboratory? As shown in Fig. 1, the stability boundary for these states is bounded by $0 \leq \kappa_0 < 0.2$, which is far below the values of κ_0 explored in prior experiments. The effects of air drag are typically small compared to the drag associated with the transfer of the walker's momentum to the bath,[11]

so we may approximate $D \approx Cmg\sqrt{\rho R/\sigma}$ in Eq. (2). Combining the formulas in Eqs. (2) and (5), we thus obtain the approximation

$$\kappa_0^2 \approx \frac{\sqrt{2\pi}}{3g^2 C^3}\left(\frac{\sigma}{\rho}\right)^{3/2}\frac{k_F^5 R^{3/2}}{3k_F^2\sigma/(\rho g)+1}\sqrt{\frac{\nu_e}{T_F}}\sin\Phi. \quad (8)$$

For deep-water capillary waves, $k_F \propto f^{2/3}$, so the value of κ_0 could readily be decreased by decreasing the forcing frequency f. Indeed, Protière et al.[25] have observed walkers using a forcing frequency $f = 35\,\mathrm{Hz}$ and a silicone oil with kinematic viscosity $\nu = 100\,\mathrm{cSt}$, which corresponds to the value $\kappa_0 = 0.45$ for $R = 0.4\,\mathrm{mm}$ and $\sin\Phi = 0.2$. While this value of κ_0 is still too large to support spin states, one might hope to find stable spin states by further decreasing the forcing frequency.

IV. CONCLUSIONS

We have explored the possibility of realizing a hydrodynamic analog of the classical model of the electron.[26,27] We have developed a generalized pilot-wave framework in order to demonstrate that the innermost $n = 0$ spin states are theoretically stable, even if not readily accessible in the laboratory. These states are stable provided the dimensionless mass coefficient κ_0 is sufficiently small and the dimensionless forcing acceleration Γ is sufficiently large (Fig. 1). This regime could possibly be accessed in the laboratory by decreasing the bath's forcing frequency f. Spin states for $n \geq 1$ are found to be unstable for all values of κ_0 and Γ. When placed in a rotating frame, the $n = 0$ spin states display an analog of the Zeeman effect (Fig. 2), wherein two orbital solutions of the same radius split into orbits with distinct radii.

Labousse et al.[15] concluded that stable $n = 0$ spin states might arise in an experimentally accessible regime; furthermore, their numerical simulations suggest the possibility of wobbling spin states. Their conclusions are based on the simulations of a discrete-time iterated map. We consider a continuous-time integro-differential equation that enables the assessment of the stability of orbital states. A future direction would be to compare our results with those of a mathematical stability analysis of spin state solutions to an iterated map.[29]

It has been shown that phase adaptation, wherein the walker's impact phase $\sin\Phi$ varies with both the forcing acceleration Γ and the instantaneous wave height h, is crucial to stabilizing the orbital[21] and promenade[22] modes for interacting pairs of walkers. We thus expect that spin states may be stabilized by phase adaptation. The effect of spatial damping on the stability of spin states is also unclear. While both effects could readily be studied by appropriate modifications of the trajectory equation (6), new parameters would necessarily be introduced, making a parametric study of spin state stability prohibitive.

In the future, we plan to conduct a complete numerical exploration of Eq. (6) for $\Omega = 0$, with the goal of identifying the parameter regimes in which wobbling spin states and other self-induced quasiperiodic trajectories arise. Such states would arise when the walker experiences a wave force sufficiently large to confine its motion. We note that the dissipation-dominated limit $\kappa_0 \to 0$ produces spin states

for the largest range of Γ. In this regime, the walker's inertia is negligible and the trajectory equation (6) is first-order in time. This parameter regime thus might be ideal for exploring other hydrodynamic quantum analogs, such as the double quantization of trajectories in radial extent and angular momentum[4,29,30] emerging in the presence of applied potentials. The discrete-time theoretical model of Durey and Milewski[29] represents an efficient means to address this class of problems.

APPENDIX: STABILITY OF ORBITAL SOLUTIONS

Consider a walker executing a circular orbit of radius r_0 and orbital frequency ω in a frame rotating with frequency Ω. Oza *et al.*[13] linearized the integro-differential trajectory equation (6) around this orbital state and showed that the eigenvalues of the linear stability problem correspond to the roots of the function

$$F(s) = (1 - e^{-2\pi(s+1)/|\omega|})[A(s)D(s) + B(s)C(s)], \quad (A1)$$

where

$$A(s) = \kappa_0(1-\Gamma)s^2 + s - \kappa_0(1-\Gamma)\omega^2 - \Omega\omega$$
$$- \frac{2}{(1-\Gamma)^2|\omega|}\mathcal{I}\left[f(t)\cos^2\frac{t}{2} + g(t)\sin^2\frac{t}{2}\right]$$
$$- \frac{2}{(1-\Gamma)^2|\omega|}\mathcal{L}\left[g(t)\sin^2\frac{t}{2} - f(t)\cos^2\frac{t}{2}\right],$$
$$B(s) = [2\omega\kappa_0(1-\Gamma) + \Omega]s - [\kappa_0(1-\Gamma)\omega + \Omega]$$
$$- \frac{1}{(1-\Gamma)^2\omega}\mathcal{L}\left\{[f(t) + g(t)]\sin t\right\},$$
$$C(s) = [2\omega\kappa_0(1-\Gamma) + \Omega]s + 2\omega + \kappa_0(1-\Gamma)\omega + \Omega$$
$$- \frac{1}{(1-\Gamma)^2\omega}\mathcal{L}\left\{[f(t) + g(t)]\sin t\right\},$$
$$D(s) = \kappa_0(1-\Gamma)s^2 + s - 1$$
$$- \frac{2}{(1-\Gamma)^2|\omega|}\mathcal{L}\left[f(t)\sin^2\frac{t}{2} - g(t)\cos^2\frac{t}{2}\right], \quad (A2)$$

the functions $f(t)$ and $g(t)$ are defined as

$$f(t) = \frac{J_1\left(2r_0\sin\frac{t}{2}\right)}{2r_0\sin\frac{t}{2}}e^{-t/|\omega|}, \quad g(t) = J_1'\left(2r_0\sin\frac{t}{2}\right)e^{-t/|\omega|}, \quad (A3)$$

and the integral operation $\mathcal{I}[f]$ and Laplace transform $\mathcal{L}[f]$ are defined as

$$\mathcal{I}[f] = \int_0^\infty f(t)\,dt \quad \text{and} \quad \mathcal{L}[f] = \int_0^\infty f(t)e^{-st/|\omega|}\,dt. \quad (A4)$$

We introduce the variable $z = (s+1)/|\omega|$ and define the corresponding function $\tilde{F}(z)$ as $\tilde{F}(z) = F(s)$. To compute $\tilde{F}(z)$ efficiently, we use the fact that, if $q(t)$ is a 2π-periodic
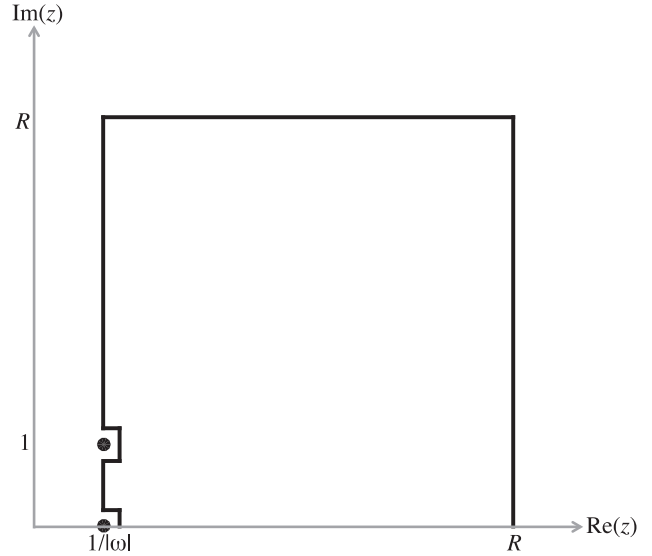

FIG. 3. Contour L in the complex z-plane used to evaluate Eq. (A6). The contour is oriented counterclockwise, and the trivial roots of $\tilde{F}(z)$ at $z = 1/|\omega|$ and $z = 1/|\omega| + i$ are indicated by the black dots. In principle, one should take the limit $R \to \infty$; in practice, we take $R = 20$ for the numerical calculations in this paper.

function of t,

$$\mathcal{I}\left[q(t)e^{-t/|\omega|}\right] = \frac{1}{1 - e^{-2\pi/|\omega|}}\int_0^{2\pi} q(t)e^{-t/|\omega|}\,dt$$

$$\text{and} \quad \mathcal{L}\left[q(t)e^{-t/|\omega|}\right] = \frac{1}{1 - e^{-2\pi z}}\int_0^{2\pi} q(t)e^{-zt}\,dt. \quad (A5)$$

The integrals in Eq. (A2) may thus be computed on the finite interval $[0, 2\pi]$. Oza *et al.*[13] also showed that $F(s)$ has trivial roots at $s = 0$ and $s = \pm i\omega$ (or $z = 1/|\omega|$ and $z = 1/|\omega| \pm i$) which correspond, respectively, to the rotational and translational invariance of the orbital solution.

The orbital solution is stable if and only if all of the nontrivial roots of $F(s)$ satisfy $\text{Re}(s) < 0$, or, equivalently, the roots of $\tilde{F}(z)$ satisfy $\text{Re}(z) < 1/|\omega|$. We assess the stability of the orbital solution by employing the argument principle from complex analysis. Specifically, we numerically compute the quantity

$$N = \text{Im}\left[\frac{1}{\pi}\int_L \frac{\tilde{F}'(z)}{\tilde{F}(z)}\,dz\right], \quad (A6)$$

where we use the fact that $\tilde{F}(z)$ is real-valued on the real axis $\text{Im}(z) = 0$, and the contour L is shown in Fig. 3. The solution is stable if $N = 0$ and is unstable otherwise. An extension of this method, as proposed by Delves and Lyness,[31] allows us to also locate the unstable eigenvalues, as was necessary for Fig. 2.

[1]A. Eddi, E. Fort, F. Moisy, and Y. Couder, "Unpredictable tunneling of a classical wave-particle association," Phys. Rev. Lett. **102**, 249491 (2009).
[2]E. Fort, A. Eddi, J. Moukhtar, A. Boudaoud, and Y. Couder, "Path-memory induced quantization of classical orbits," Proc. Natl. Acad. Sci. U.S.A. **107**, 17515–17520 (2010).
[3]A. Eddi, J. Moukhtar, S. Perrard, E. Fort, and Y. Couder, "Level splitting at macroscopic scale," Phys. Rev. Lett. **108**, 264503 (2012).

[4]S. Perrard, M. Labousse, M. Miskin, E. Fort, and Y. Couder, "Self-organization into quantized eigenstates of a classical wave-driven particle," Nat. Commun. **5**, 3219 (2014).

[5]D. M. Harris, J. Moukhtar, E. Fort, Y. Couder, and J. W. M. Bush, "Wave-like statistics from pilot-wave dynamics in a circular corral," Phys. Rev. E **88**, 011001(R) (2013).

[6]J. W. M. Bush, "Pilot-wave hydrodynamics," Ann. Rev. Fluid Mech. **47**, 269–292 (2015).

[7]J. W. M. Bush, "The new wave of pilot-wave theory," Phys. Today **68**(8), 47–53 (2015).

[8]D. M. Harris and J. W. M. Bush, "Drops walking in a rotating frame: From quantized orbits to multimodal statistics," J. Fluid Mech. **739**, 444–464 (2014).

[9]C. Cohen-Tannoudji, B. Diu, and F. Laloë, *Quantum Mechanics* (John Wiley & Sons, 1977).

[10]J. Moláček and J. W. M. Bush, "Drops bouncing on a vibrating bath," J. Fluid Mech. **727**, 582–611 (2013).

[11]J. Moláček and J. W. M. Bush, "Drops walking on a vibrating bath: Towards a hydrodynamic pilot-wave theory," J. Fluid Mech. **727**, 612–647 (2013).

[12]A. U. Oza, R. R. Rosales, and J. W. M. Bush, "A trajectory equation for walking droplets: Hydrodynamic pilot-wave theory," J. Fluid Mech. **737**, 552–570 (2013).

[13]A. U. Oza, D. M. Harris, R. R. Rosales, and J. W. M. Bush, "Pilot-wave dynamics in a rotating frame: On the emergence of orbital quantization," J. Fluid Mech. **744**, 404–429 (2014).

[14]M. Labousse, A. U. Oza, S. Perrard, and J. W. M. Bush, "Pilot-wave dynamics in a harmonic potential: Quantization and stability of circular orbits," Phys. Rev. E **93**, 033122 (2016).

[15]M. Labousse, S. Perrard, Y. Couder, and E. Fort, "Self-attraction into spinning eigenstates of a mobile wave source by its emission back-reaction," Phys. Rev. E **94**, 042224 (2016).

[16]M. Faraday, "On a peculiar class of acoustical figures, and on certain forms assumed by groups of particles upon vibrating elastic surfaces," Philos. Trans. R. Soc. Lond. **121**, 299–340 (1831).

[17]A. Eddi, E. Sultan, J. Moukhtar, E. Fort, M. Rossi, and Y. Couder, "Information stored in Faraday waves: The origin of a path memory," J. Fluid Mech. **674**, 433–463 (2011).

[18]K. Kumar, "Linear theory of Faraday instability in viscous liquids," Proc. R. Soc. A **452**, 1113–1126 (1996).

[19]P. A. Milewski, C. A. Galeano-Rios, A. Nachbin, and J. W. M. Bush, "Faraday pilot-wave dynamics: Modelling and computation," J. Fluid Mech. **778**, 361–388 (2015).

[20]A. P. Damiano, P.-T. Brun, D. M. Harris, C. A. Galeano-Rios, and J. W. M. Bush, "Surface topography measurements of the bouncing droplet experiment," Exp. Fluids **57**, 163 (2016).

[21]A. U. Oza, E. Siéfert, D. M. Harris, J. Moláček, and J. W. M. Bush, "Orbiting pairs of walking droplets: Dynamics and stability," Phys. Rev. Fluids **2**, 053601 (2017).

[22]J. Arbelaiz, A. U. Oza, and J. W. M. Bush, "Promenading pairs of walking droplets: Dynamics and stability," Phys. Rev. Fluids **3**, 013604 (2018).

[23]S. Protière, A. Boudaoud, and Y. Couder, "Particle-wave association on a fluid interface," J. Fluid Mech. **554**, 85–108 (2006).

[24]A. U. Oza, Ø. Wind-Willassen, D. M. Harris, R. R. Rosales, and J. W. M. Bush, "Pilot-wave hydrodynamics in a rotating frame: Exotic orbits," Phys. Fluids **26**, 082101 (2014).

[25]S. Protière, Y. Couder, E. Fort, and A. Boudaoud, "The self-organization of capillary wave sources," J. Phys. Condens. Matter. **17**, S3529–S3535 (2005).

[26]E. Schrödinger, "Uber die kräftefreie Bewegung in der relativistischen Quantenmechanik," "On the free movement in relativistic quantum mechanics" (in English), Sitz. Preuss. Akad. Wiss. Phys. Math. Kl. **24**, 418–428 (1930) OCLC number 881393652.

[27]A. Burinskii, "The Dirac-Kerr-Newman electron," Gravit. Cosmol. **14**, 109–122 (2008).

[28]D. Bohm, "A suggested interpretation of the quantum theory in terms of "hidden" variables. I," Phys. Rev. **85**, 166–179 (1952).

[29]M. Durey and P. A. Milewski, "Faraday wave-droplet dynamics: Discrete-time analysis," J. Fluid Mech. **821**, 296–329 (2017).

[30]K. M. Kurianski, A. U. Oza, and J. W. M. Bush, "Simulations of pilot-wave dynamics in a simple harmonic potential," Phys. Rev. Fluids **2**, 113602 (2017).

[31]L. M. Delves and J. N. Lyness, "A numerical method for locating the zeros of an analytic function," Math. Comput. **21**, 543–560 (1967).